CHAPTER 51

CHARACTERISTICS OF OSCILLATORY FLOW OVER RIPPLE MODELS

Kiyoshi Horikawa[1] F.ASCE
Syunsuke Ikeda [2] M.ASCE

ABSTRACT

The results of extensive laboratory investigations on the oscillatory flow over ripple models were presented. The ripple models were installed in an oscillatory flow flume. A two-dimensional lasser doppler velocimeter was utilized to measure the fine structure of flows in the vicinity of the whole length of a ripple model which was induced by various types of oscillatory flow. The results of measurements were displayed in the form of distributions of mean fluid velocity, stationary velocity, fluid turbulence intensity and Reynolds stress. By using these data the characteristics of oscillatory flow, such as the formation and decay of vortices, the generation of stationary velocity and the variation of kinematic eddy viscosity were discussed.

INTRODUCTION

More than 40 years ago Bagnold (1946) made his laboratory investigations on the oscillatory flow over sand ripples by oscillating the arced bottom harmonically through stil water. Since then considerable amount of laboratory investigations have been attempted to clarify the stated phenomena in connection with various subjects, such as the mechanism of ripple formation, the ripple geometry, the sediment transport in the vicinity of sand ripples, and the wave energy dissipation due to the existence of sand ripples.

1. Professor, Department of Foundation Engineering, Saitama University, 255 Shimo-Okubo, Urawa, Saitama 338, Japan. Professor Emeritus, The University of Tokyo.
2. Professor, Department of Civil Engineering, Tokyo Institute of Technology, 2-12-1 O-okayama, Meguro-Ku, Tokyo 152, Japan.

During the last decade the laser doppler velocimeters (LDV) have been adopted together with the data acquisition system to display precisely the fields of mean velocity and turbulence intensity within the domain which was set for the measurement (Du Toit et al.,1980 ; Sawamoto et al.,1981 ; Sato, 1987 ; Sleath, 1987).

Therefor our knowledge on the fine structure of oscillatory boundary layer flow has been deepend during the last decade. The most remarkable phenomenon observed around sand ripples is the generation of vortices separated from a certain location near the ripple crest. It has been realized that the life of vortices from generation to decay is an important element for determining the structure of flow field which has strong influence on the suspension of sediment near the sand ripple and on the decay of wave energy (Ikeda, et al.,1989). In order to clarify more the detailed structures of the oscillatory boundary layer flow, we have continued to carry out a series of laboratory investigations in an oscillatory flume in which sand ripple model was installed. The model of sand ripples has a characterized shape with a sharpened crest as shown in Figure 1. The reason why we adopted such a peculia sharp-crested ripple, which is quite different from the actual sand ripples with a rounded crest, is, for the sake of simplicity, to fix the separation point of flow at a definite point; that is at its crest (Longuet-Higgins, 1981).

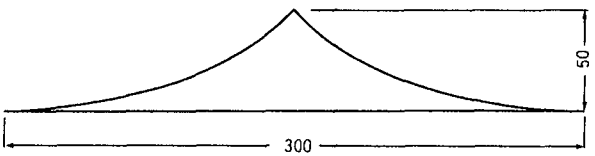

Fig.1 Profile of the ripple model. (unit:mm)

EXPERIMENTAL FACILITIES AND PROCEDURES

An oscillatory flow flume with 13 m in length and 0.3 m x 0.3 m in cross-section was used for the laboratory experiment, the observation section of which was 2 m long and was made of glass except the flume bottom (Figure 2). The oscillatory fluid motion was produced by a piston driven by a DC-motor, and the maximum amplitude of the fluid motion was 70 cm. The period of fluid oscillation was variable between 1 s and 20 s.

The height and length of the ripple model were selected to be 5 cm and 30 cm, respectively (Figure 1).

The surface of the ripple was finished smoothly. Seven of model ripples were placed at the test section, among which the region between the 3rd and the 4th crests was selected for the precise velocity measurement. We took four cases as experimental runs as shown in Table 1. The periods of test runs varied from 3 s to 9 s. The measuring points were decided to be 316 points in total as indicated in Figure 3. That is to say, one wave length of ripple was divided into 12 sections, and the vertical spacing were taken to be 5 mm, 10 mm and 20 mm from the bottom to a certain elevation as shown in Figure 3.

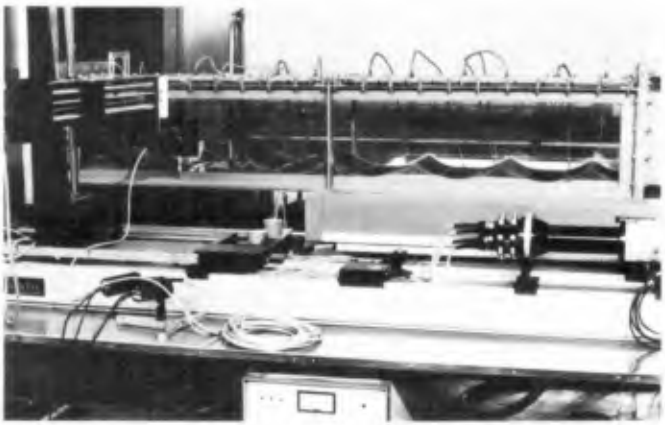

Fig.2 Exprimental apparatus.

Table 1 Experimental conditions.

Run	1	2	3	4
T(s)	9.0	6.0	3.0	6.0
$\hat{U}$(cm/s)	13.9	20.9	20.9	10.5
Re	2.7×10^4	4.2×10^4	2.1×10^4	1.1×10^4

$\hat{U}$: amplitude of the oscillatory flow velocity

$Re = \frac{\hat{U}a}{\nu} = \frac{\hat{U}^2 T}{2\pi\nu}$: Reynolds number

a : amplitude of the oscillatory flow motion
ν : kinematic viscosity of fluid

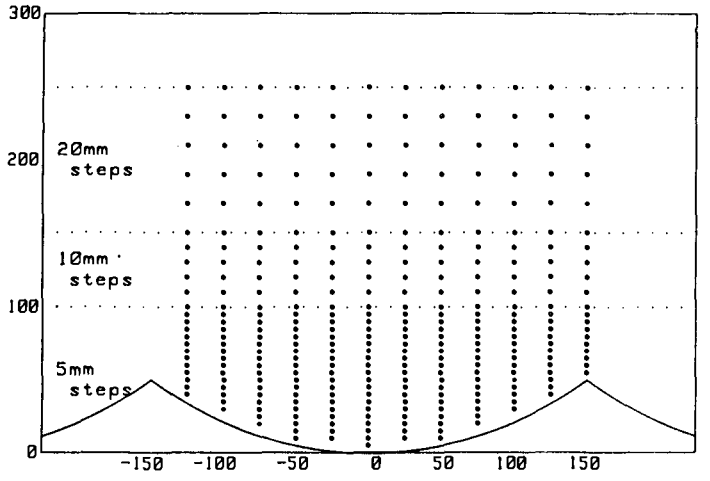

Fig.3 Data sampling points.

At each measuring point the velocity measurement was made for 30 cycles of waves by using a 2-D LDV. The lens of the velocimeter was moved by a 3-D traverse facility controlled by a mini-computer with a minimum displacement of 0.5 mm. Thus horizontal and vertical velocity components were measured. The commencement of data sampling was controlled by an electric signal generated at the piston. The phase 0 was selected at the instant when the movement of the piston became stationary, i.e. the cross-sectionally averaged fluid velocity became zero. The sampling time was selected to be 0.0195 s, during which 5 data were obtained. Therefore, 150 data were acquired for one phase at a measuring point. The interval of the sampling phases was $\pi/8$. The local mean fluid velocity, the intensity of fluid turbulence, the Reynolds stress, the kinematic eddy viscosity and the stationary velocity components were calculated by using 150 data at one phase and at one point and displayed in a graphical form.

RESULTS OF LABORATORY INVESTIGATION AND DISCUSSION

Mean Fluid Velocity

The boundary layer developed along a ripple surface can be divided into two parts. The first one is the inner boundary layer or the Stokes layer existing very close to the bottom boundary, where the fluid flow is strongly controlled by fluid viscosity. The second one is the outer boundary layer where the flow structure is characterized by the behavior of organized vortices

separated from the crest of the ripples. The thickness of the inner boundary layer is very thin with the order of $\sqrt{\nu T}$, where ν is the kinematic viscosity of fluid and T is the oscillation period.

Variation of the mean velocity fields during the phases 0 to $7\pi/8$ for Run 3 was illustrated in Figure 4 with a time interval of $\pi/8$. Through the careful observation of time variation of velocity field illustrated in Figure 4, the behavior of an organized vortex covering its growing and then decaying processes can be realized. This phenomenon is a remarkable feature of the outer boundary layer of the oscillatory flow.

In order to clarify the characteristic behavior of the flow in the inner boundary layer, the velocity distribution at the section just above a ripple crest was measured. The reason is that the thickness of the boundary layer at the crest must be specified in predicting the circulation of the vortices. Based on the result of velocity measurement, the temporal variation of the boundary layer thickness for two selected cases were plotted as shown in Figure 5. It is clearly noticed that the thickness reduces considerably at flow accelerating phases, while the thickness tends to increase at decelerating phases. Even though the boundary layer thickness shows such a temporal variation as stated above, the temporaly averaged value of the thickness is reasonably well described by $\sqrt{\nu T}$ as seen in this figure.

It has been predicted theoretically that stationary cells are generated in the outer boundary layer of the oscillatory flows over a wavy boundary. In our study the stationary velocity component was derived by averaging the fluid velocity for one period of oscillatory flow at each measuring point. The result for Runs 2 and 3 were drown in Figure 6, from which it can be clearly observed that two stationary cells were generated. The maximum steady flow velocity seemes to occur near the bottom close to the ripple crests. The ratio of the maximum steady velocity to the velocity amplitude of the undisturbed flow, $\hat{U}$, was calculated and shown in Table 2. From this table it is found that the stated ratio was affected by the period of fluid oscillation. For T = 3 s, the ratio was about 0.76, while it was about 0.58 for T = 9 s. These results indicate that the magnitude of stationary velocity is very large near the bottom. This fact suggests that the stationary cell has an important role in amplifying the height of ripples. It can also be observed that the

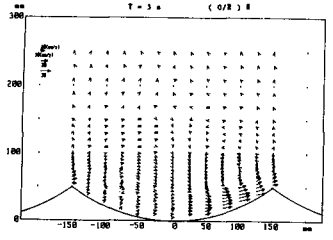
(a)

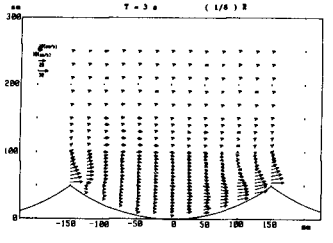
(b)

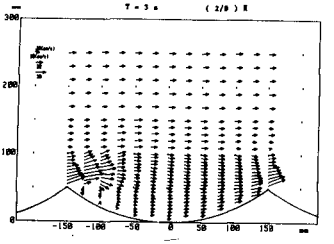
(c)

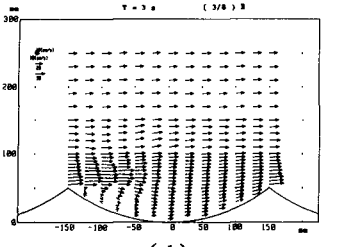
(d)

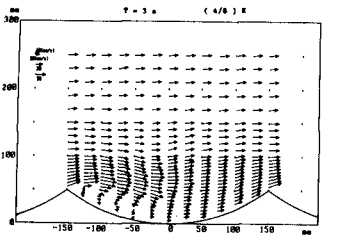
(e)

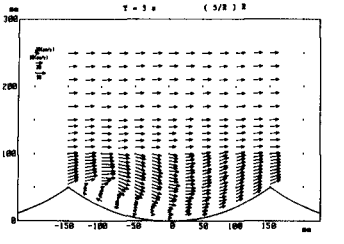
(f)

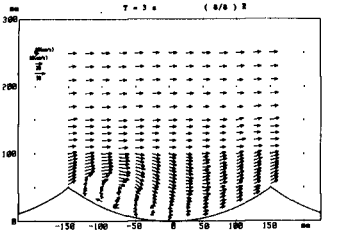
(g)

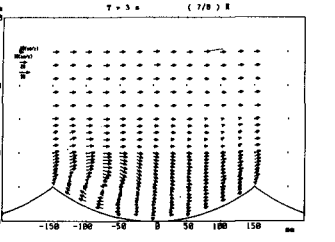
(h)

Fig.4 Distributions of temporally averaged fluid velocity for Run 3.

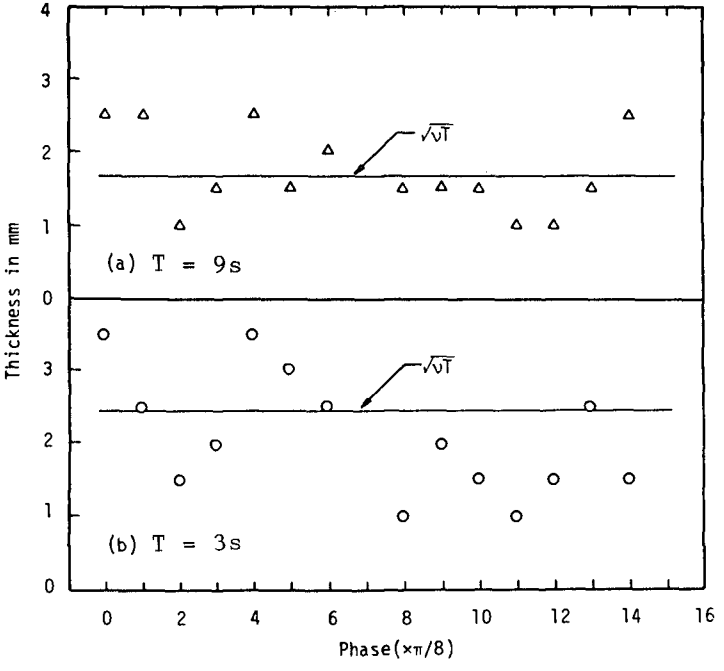

Fig.5 Temporal variation of the inner boundary layer thickness above the ripple crest.

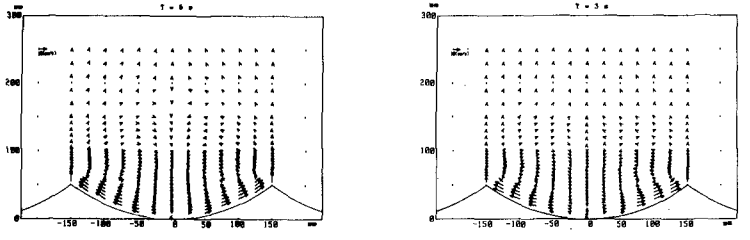

(a) (b)

Fig.6 Stationary velocity distributions for (a) Run 2 and (b) Run 3.

Table 2 Maximum speed of stationary current, V_{max}.

T (s)	3	6	9
$\hat{U}$ (cm/s)	20.9	20.9	13.9
V_{max} (cm/s)	15.8	13.3	8.02
$\frac{V_{max}}{\hat{U}}$	0.76	0.64	0.58

stationary cells are significantly correlated with the vortices which seem to strengthen the stationary velocity component compared with that predicted for rolling grain ripples. The laboratory data at the University of Tokyo (Hamamoto, et al.,1982) obtained by using a sinusoidal shape bottom boundary indicated that the questioned ratio was about 0.3, considerably smaller than the present results. Therefore the circulation of the vortices generated over the round-crested ripples is expected to be smaller than that over sharp-crossted ripples. The second series of our experiment using a round-crested ripple model, which is now going on, is expected to give more definte conclusions on this subject.

Fluid Turbulence Intensity

The intensity of fluid turbulence was calculated by using 150 data for each velocity component obtained for each phase at each measuring point. Figure 7 shows the variation of the vertical distribution of turbulence intensity expressed in the form of RMS value during a half-cycle of fluid oscillation. The intensity of fluid turbulence was slightly large in the area where the vortex separated from the right hand side crest in the preceding period was still existing at the phase of (0/8)π and gradually attenuated in due course. On the contrary to this, the turbulence intensity in the right hand side area of the left crest increased and the area with large turbulence intensity increased its size. The turbulence intensity reached the maximum at the phase $4\pi/8$ near the center of the vortex, the value of which became as large as 80 % of the velocity amplitude of the undisturbed oscillatory flow, $\hat{U}$. The fluid turbulence was convectively transported toward the down stream, and prevailed in almost all over the boundary layer between the two neighbouring crests at the phase $6\pi/8$. The turbulence intensity became to decrease its magnitude at

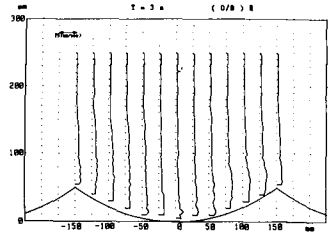

(a)

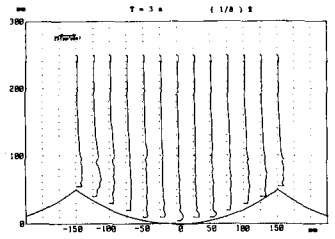

(b)

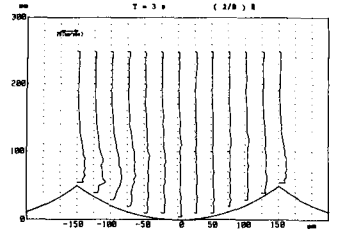

(c)

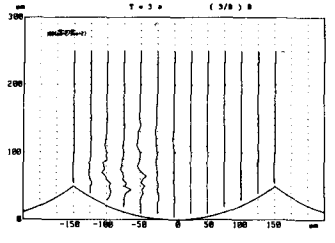

(d)

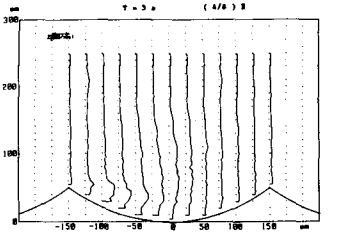

(e)

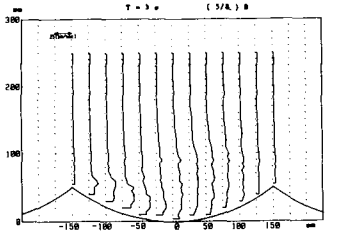

(f)

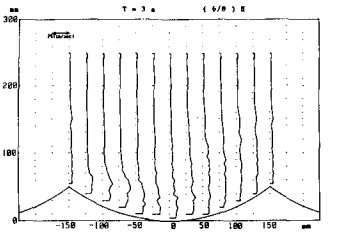

(g)

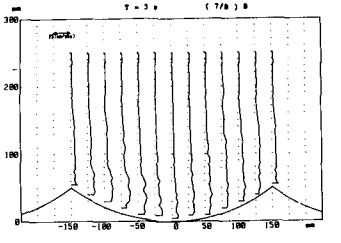

(h)

Fig.7 Distributions of the fluid turbulence intensity for Run 3.

the phase $7\pi/8$, but the intensity still kept the level of 60 % of the velocity amplitude.

The Reynolds Stress

The kinematic Reynolds stress, $-\overline{u'v'}$, was also obtained as depicted in Figure 8. The distributions of the Reynolds stress show more clearly the effect of the vortices on the turbulent fluid. At the phase $(0/8)\pi$, the Reynolds stress was almost zero everywhere except the limited region on the right hand side where a weak negative Reynolds stress was observed corresponding to the vortex shed from the right hand side ripple crest. At the phase $\pi/8$ a weak positive Reynolds stress began to appear in the downstream of the left crest corresponding to the release of vorticity from the crest. The Reynolds stress increased very rapidly at the phase $2\pi/8$, where the value was positive below the prescribed streamline with the maximum fluid velocity and negative above the streamline. The region of large Reynolds stress moved downstream, and the absolute value of the Reynolds stress reduced considerably at the phase $3\pi/8$. This reduction corresponds to the fact that the vertical distribution of mean fluid velocity became more uniform near the crest. The Reynolds stress took positive value almost everywhere, and reached its maximum at the phase $4\pi/8$ in the vortex region.

The Reynolds stress begans to appear in the region above the ripple trough, and was probably induced by a large fluid velocity transported convectively from the left hand side ripple crest. The maximum fluid velocity at the trough located at about $y = 70$ mm, below and above which the Reynolds stress was positive and negative respectively. The overall Reynolds stress gradually decreased toward the phase $7\pi/8$.

These observations reveal that the Reynolds stress is significantly correlated with the release of the vorticity from the ripple crest and is essentially zero in the area where the vorticity is not supplied from the ripple crest even if the turbulence intensity has non-zero value there.

Kinematic Eddy Viscosity

The kinematic eddy viscosity, ε_ν, was calculated at a few fixed points as well as at the center of the organized vortex. Because the generation of the Reynolds stress is significantly correlated with the vortex formation as revealed previously, the temporal variation of the kinematic eddy viscosity at the vortex

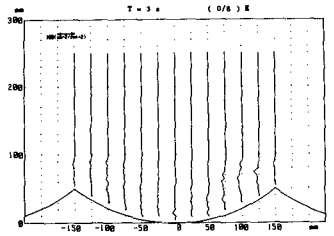

(a)

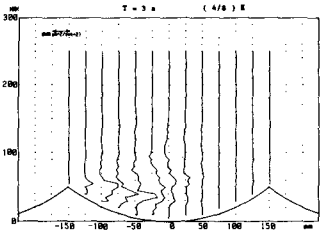

(e)

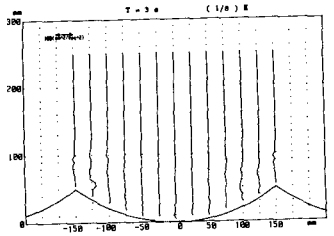

(b)

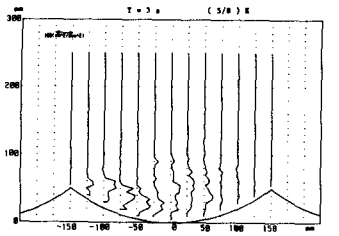

(f)

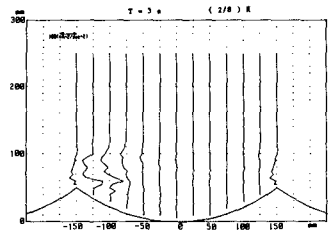

(c)

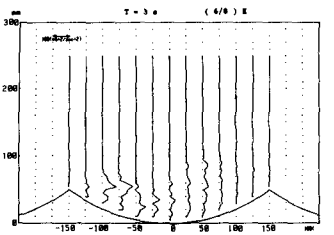

(g)

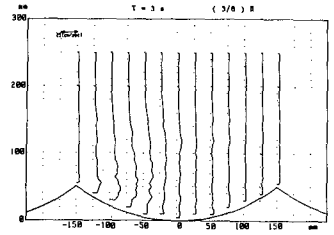

(d)

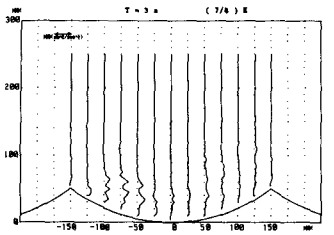

(h)

Fig.8 Distribution of kinematic Reynolds stress for Run 3.

center will be described here. The results were given in Figure 9, in which the kinematic eddy viscosity was calculated from the raw data, without smoothing, of the distribution of the fluid velocity and the Reynolds stress. A large variety of the kinematic eddy viscosity with time is almost in accordance with the undisturbed oscillatory flow for each case. It is clearly seen that the kinematic eddy viscosity increased linearly with phase until the phases $4\pi/8$ and $12\pi/8$, at which the fluid velocity reached its maximum. The kinematic eddy viscosity, then, decreased rather gradually, and therefore it indicated a slightly unsymmetrical distribution with respect to the phase. The above feature was common for each run. The distribution of the kinematic eddy viscosity non-dimensionalized by the velocity amplitude of the undisturbed oscillatory flow and the ripple height, , becomes nearly identical as shown in Figure 10. The results obtained here suggests that the assumption of constant kinematic eddy viscosity does not hold in the present type of flow, and a turbulent model such as two equation model must be employed to predict the flow field.

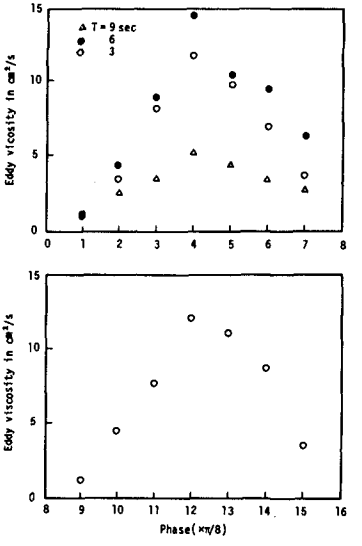

Fig.9 Temporal variations of kinematic eddy viscosity at the vortex center.

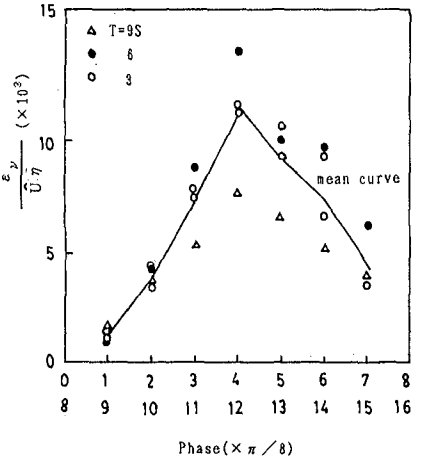

Fig.10 Temporal variation of the non-dimensionalized kinematic eddy viscosity.

CONCLUSIONS

A detailed measurement was performed for the oscillatory boundary layer flow over a shap-crested ripple model by using a 2-D LDV cotrolled by a computer. The conclusions are summarized as follows:

(1) The oscillatory boundary layer over a ripple model is separated into two parts ; the inner and the outer boundary layers. The thickness of the inner boundary layer is well expressed by $\sqrt{\nu T}$. The feature of the outer boundary layer is characterised by the organized vortices, and the growth of the vortices has a phase-lag against the undisturbed main flow.

(2) The stationary velocity component constitutes two cells between two ripple crests, the distribution of which is similar regardless of the test conditions. The flow is moving toward the crests, and the velocity is very large near the bottom boundary close to the ripple crests.

(3) The fluid turbulence is found to be closely correlated with the vortices. The generation of the Reynolds stress is limited essentially within the vortex region. Some minor part of the vortices is convectively transported downstream, and yields weak Reynolds stress there.

(4) The kinematic eddy viscosity obtained at the near-center of the organized vortices reveals that it varies sinusoidally in accordance with the oscillatory flow. The variation of the kinematic eddy viscosity with respect to the phase is similar to the other regardless of the test conditions reported herein.

(5) The three-dimensional structure of the oscillatory boundary layer is still left as a future subject.

ACKNOWLEDGMENT

This study has been supported by the Grant-in-Aid for Scientific Research from the Ministry of Education and Culture of Japan (Grant No.01460180).

REFERENCES

Bagnold, R. A. : Motion of waves in shallow water, Interaction between waves and sand bottoms, Proc. Royal Society, London, A187, pp.1-18, 1946.

Ikeda, S., S. Kizaki, S. Ishii and S. Kuribayashi : Flow near sand ripples and dissipation of wave energy, Coastal Eng. in Japan, Vol.32, No.1, pp.15-36, 1989.

Du Toit, C. G. and J. F. A. Sleath : Velocity measurements close to rippled beds in oscillatory flow, J. Fluid Mech., Vol.112, pp.71-96, 1981.

Hamamoto, K., N. Mimura and A. Watanabe : Experimental study on oscillatory boundary layer over sand ripples (2), Proc. 29th Japanese Coastal Eng. Conf., JSCE, pp.254-258, 1982 (in Japanese).

Longuet-Higgins, M. S. : Oscillating flow over steep sand ripples, J. Fluid Mech., Vol.107, pp.1-35, 1981.

Sato, S. : A Fundamental Study on Shoaling and Velocity Field Structure of Water Waves in the Nearshore Zone, Dr. Thesis. The University of Tokyo, Feb. 1987.

Sawamoto, M., T. Yamashita and M. Kitamura : Distributions of turbulent intensity and suspended sediment concentration, Proc. 28th Japanese Coastal Eng. Conf., pp.232-236, 1981 (in Japanese).

Sleath, J. F. : Turbulent oscillatory flow over rough beds, J. Fluid Mech., Vol.182, pp.369-409, 1987.